GNSS Measurement Exclusion and Weighting with a Dual Polarized Antenna: The FANTASTIC project

Daniel Egea-Roca*, Antonio Tripiana-Caballero*, José A. López-Salcedo*, Gonzalo Seco-Granados*
Wim De Wilde#, Bruno Bougard#, Jean-Marie Sleewaegen# and Alexander Popugaev$
* *Department of Telecommunications and Systems Engineering, IEEC-CERES, Universitat Autònoma de Barcelona (UAB), Spain*
# *Septentrio, Leuven, Belgium*
$ *Fraunhofer IIS, Erlangen, Germany*

***Abstract*—The widespread use of global navigation satellite systems (GNSSs) in professional applications has posed very stringent requirements in terms of adoption and absolute performance. Unfortunately, current GNSS performance is not enough to fulfill the requirements of professional applications like farming, critical timing infrastructures or autonomous driving. In order to boost the adoption of these applications, the European GNSS agency (GSA) launched the FANTASTIC project aimed at enhance robustness and accuracy of GNSS in harsh environments. We will focus in this paper on the part related with the development of a weighting and exclusion function with a dual circularly polarized antenna. The idea is to reduce the effects of multipath by weighting and/or excluding those measurements affected by multipath. The capabilities of a dual polarized antenna to sense multipath will be exploited to define an exclusion threshold and to provide the weights. Real-world experiments will be shown assessing the improvements of applying the developed technique in the positioning solution.**

***Index Terms*—Dual polarization, multipath mitigation, weighting, exclusion.**

I. Introduction

Professional applications based on global navigation satellite systems (GNSSs) are getting a significant boost in terms of adoption and absolute performance, mainly driven by the growing number of satellites and signals. Furthermore, the wide use of correction services, like EGNOS, precise point positioning, regional and nationwide real time kinematics (RTK) networks, offers sub-decimeter accuracy. Nevertheless, this cutting edge accuracy is not enough for a large variety of emerging applications posing very stringent requirements. These applications include the control of driverless machineries in precision farming, autonomous vehicles, and GNSS-based systems resilient to interference, just to mention a few.

For the above reason, the FANTASTIC project was launched in order to develop enabling technologies that allow a leap of professional applications. One of the main tasks of the FANTASTIC project is to demonstrate the improvement of the RTK processing in harsh environments, where the received signal is likely to be corrupted by obstacles and foliage. To enhance robustness, the work focuses on a dual circularly polarized multi-band antenna, a new strategy to combine inertial measurement unit (IMU) and GNSS measurements and on interference mitigation algorithms. This paper will focus on the part corresponding to the antenna. It has two orthogonal polarization outputs (Right-Hand Circular Polarization (RHCP) and Left-Hand Circular Polarization (LHCP) components). Since GNSS satellites transmit RHCP signals, the underlying idea with this configuration is that multipath may affect both the RHCP and the LHCP components, while the direct or genuine signal appears only on the RHCP component.

The aim of this paper is to show the developed function in the FANTASTIC project to weight and exclude observables based on the above concept. The goal of the proposed weighting and exclusion (WE) function is to reduce the effects of multipath into the PVT solution. Actually, there are many methods to do so, ranging from the classical narrow or strobe correlators [1] to more sophisticated techniques such as the MEDLL [2]. These techniques are either not designed to mitigate carrier phase effects or are usually too complex to be implemented in mass-market receivers. Other schemes include site-dependent techniques trying to model the multipath propagation with in-site multipath calibrations [3] or with the use of external information such as cameras [4]. Unfortunately, these techniques are only suited to static receivers with very specific multipath propagation or they need additional hardware/components that are not usually available in mass-market receivers.

Furthermore, none of the techniques listed above completely eliminate the effects of multipath or suit all GNSS applications. The most effective techniques are those based on antenna arrays [5], which can cover most multipath situations. Nevertheless, antenna arrays are often not suited in some kinematic applications due to the size of the array, which is usually bulky. In this regard, multipath mitigation techniques using dual polarization antennas may provide a good alternative due to the reduction of size, as they have the same size as a single antenna element. The first studies of dual polarization antennas for GNSS multipath mitigation can be found in [6]–[8], which consider in-lab experiments or simulation demonstrations.

It was not until some years later, though, that real-world conditions were analyzed in [9]–[11]. These works demonstrated for the first time the capability of dual polarization antennas to detect NLOS and its improvements on the positioning accuracy under real working conditions. Nonetheless, for the best of the authors' knowledge, there is no literature available evaluating the case of RTK phase-based positioning, and for the application of a weighting function there is only the work in [12]. Based on these observations, the contribution of this paper is twofold. On the one hand, we illustrate the design of an exclusion function with a dual polarized antenna and its effects on the performance of the RTK phase-based positioning in real-world conditions. On the other hand, we introduce a novel weighting function based on a dual-polarized antenna.

The rest of the paper is organized as follows: Section II introduces the set-up and scenarios considered for the measurement collection campaign. We also show some preliminary results before entering into details of the proposed WE function in Section III. Finally, Section IV shows the PVT results after applying the proposed WE function, while Section V concludes the paper.

II. Measurement Collection Campaign

Multipath propagation is one of the main limiting factors on the accuracy of GNSS for professional applications operating in harsh environments like dense urban areas or foliage zones. In particular, the case when the direct LOS signal is not present, known as NLOS signal reception, is very dangerous because they can induce very

Fig. 1. Benign test scenario. Static recording attempted to minimize multipath.

Fig. 2. Foliage test scenario. Static recording under trees.

Fig. 3. Urban test scenario. Static recording between two buildings.

Fig. 4. Dynamic test scenario. Truth (pink) and computed (blue) trajectory.

large errors depending on the distance of the reflector. These effects can be sensed by using a dual polarized antenna, as we show in this section by introducing the collection campaign carried out within the framework of the FANTASTIC project.

This data collection campaign is necessary and very useful for the development of the proposed WE function in Section III. Specifically, the data captured includes the following recordings, each of them lasting for about 2 hours. The measurements were done during the same time slot at consecutive days. This results in a nearly identical GPS constellation behavior, because of the periodicity of GPS.

- **Benign**: Static recording at the open sky scenario shown in Fig. 1. This test is attempted to minimize multipath and to be the reference file for calibration purposes.
- **Foliage**: Static recording under dense tree canopy to capture multipath and/or diffraction, shown in Fig. 2.
- **Urban**: Static recording between two buildings (see Fig. 3). This test is attempted to capture multipath and NLOS conditions.
- **Dynamic**: Dynamic recording with a moving car in a mixed environment including open sky, forests and deep urban scenarios. Fig. 4 shows the truth trajectory of the moving car around Leuven, Belgium.

The used hardware to capture the data comprised a Septentrio AsteRx-U dual antenna multi-frequency receiver in conjunction with a dual polar multi-frequency antenna prototype developed by the Fraunhofer Institute for Integrated Circuits. The RHCP output of the antenna was connected to the main input of the receiver, while the LHCP output was connected to the auxiliary input of the receiver. The default software of the AsteRx-U receiver independently acquires and tracks satellite signals from each antenna input. This is a suitable

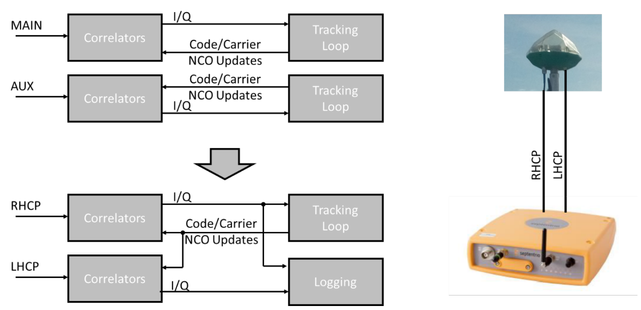

Fig. 5. Software modifications included in the AsteRx-U receiver.

approach for the normal 2D attitude use case of the receiver. However, when used for dual-polarization applications the receiver would fail to permanently monitor the polarization of the signal, as the LHCP component could only be tracked if its C/No is sufficiently high.

It is for the above reason that the receiver software was modified. Rather than having an independent tracking of the LHCP and RHCP components, the receiver only tracks the RHCP component and replicates the local code and carrier timing of the RHCP tracking to correlators which connect to the LHCP signal, as shown in Fig. 5. In this way the receiver synchronously gathers RHCP and LHCP correlation values, ensuring a permanent polarization monitoring of the signal. Both correlations were integrated over a 100-ms prediction time, after removing navigation bit modulation on both components based on the RHCP bit-detection. This was done for all satellites in view from GPS (L1CA/L2C), GALILEO (E1/E5b), GLONASS (L1CA/L2CA) and BeiDou (B1/B2). The resulting RHCP and LHCP correlations were logged on non-volatile memory in the receiver for post-processing, along with the usual raw GNSS data and differential corrections from a nearby reference station.

III. Measurement Weighting and Exclusion (WE)

This section is aimed at explaining the proposed WE function in order to reduce the effects of multipath. The development of the WE function is based on a theoretical and experimental assessment of the relation between the signal propagation conditions and the received correlation recordings at both polarizations. For instance, due to signal propagation, if the LHCP component is stronger than the RHCP one, it means that the signal has been received under NLOS conditions [11]. On the other hand, a positive RHCP to LHCP ratio in dBs but with a high signal strength in the LHCP component, would mean that the signal should be weighted down. The key question is how to derive a proper threshold to exclude measurements and a proper function that provides an appropriate value for the weight. In the following we will provide answers to these two questions.

A. Measurement exclusion

In order to evaluate the effects of multipath into the dual polarized antenna outputs it is firstly important to analyze the benign scenario. This will give us an idea of how the antenna is behaving under nominal conditions. Then, any anomalous behavior departing from the nominal one will be associated to multipath. Specifically, the ratio between the RHCP and LHCP components in the benign scenario is used to determine three different zones as done in [11] and as shown in the upper plot of Fig. 6, namely

- **Nominal** (green area): Above the 5-th percentile of the RHCP to LHCP ratio in the benign scenario. In this area the received multipath is considered to be the one received under nominal conditions and the measurements should be considered by itself (or traditional weighting).
- **Weighting area** (yellow area): In the range from 0 dB to the 5-th percentile of the RHCP to LHCP ratio in the benign scenario. In this area the received multipath is considered to be moderate (subject to a more severe multipath than in the benign scenario) and the measurements should be weighted down.
- **Exclusion area** (red area): Below the exclusion threshold. Theoretically, the exclusion threshold should be a ratio equal to 0 dB. In practice, this threshold must be calibrated. In this area, the received measurements can be considered to be obtained under NLOS conditions, thus they should be excluded.

Furthermore, the lower plot of Fig. 6 shows the three different zones together with the mean value of the RHCP to LHCP ratio, as well as the 95- and 5-th percentile curves of this ratio, as a function of the elevation angle for the data captured in the foliage scenario. The results clearly suggest the presence of multipath due to the fact that around half of the RHCP to LHCP ratio (see solid black line) measurements lie in the weighting area (yellow area), being an indicative that these data is contaminated by multipath. Moreover, more than the 5% of the data in the foliage scenario (see 5-th percentile line) is in the exclusion area (red area), thus being an indicative of NLOS conditions and very large errors.

These experiments verify the utility of the RHCP to LHCP ratio to identify the presence of multipath on GNSS signals. Now, we have to fix the exclusion threshold used to exclude the measurements. This threshold is of particular interest because it denotes the bound between the cases in which it is useful to mitigate multipath or not. Often, the latter is associated with NLOS propagation for which mitigation has no sense. In Fig. 6 this threshold is fixed to 0 dB,

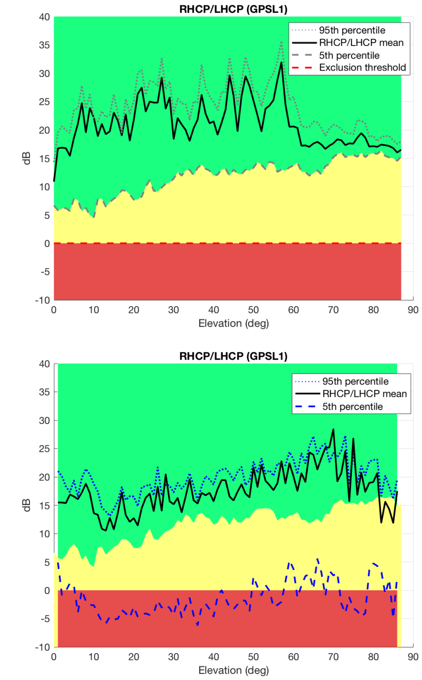

Fig. 6. Ratio between RHCP and LHCP components as a function of the elevation angle for the benign (up) and foliage (down) scenarios. Three different zones are defined: Severe multipath or NLOS (red), moderate multipath (yellow), and nominal conditions (green).

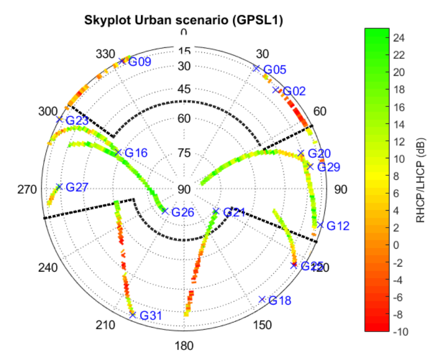

Fig. 7. Ratio between RHCP and LHCP components in a sky plot for the urban environment. Elevation masks based on the known location of the buildings in the scenario (see Fig. 3).

which is the ballpark figure for exclusion [11]. Nevertheless, due to the complexity of signal propagation, this threshold may be different. For instance, NLOS can have positive RHCP to LHCP ratio (in dB units) if the reflection incidence angle is above the Brewster's angle. In addition, LOS may have negative ratio (in dBs) in case multiple LHCP multipath rays interfere constructively.

With the aim of fine tuning the exclusion threshold we will make use of the data collected at the urban scenario. This is so because this scenario includes two buildings in know locations that block the visibility of some satellites. Using the know locations of the buildings we can draw an elevation mask, as shown in Fig. 7, in order to know when some satellite is completely blocked by the building, thus if received, it is likely to be received under NLOS conditions. In this way, taking the mean value of the RHCP to LHCP ratio of those satellites obstructed by the buildings we can estimate the value of the exclusion threshold. For instance, we see in the right plot of Fig. 7 that the satellite G31 is obstructed by the southern building from an elevation of 60°. Doing so, the selected threshold for the exclusion zone is equal to -1 dB.

B. Measurement weighting

The exclusion of measurements obtained under NLOS conditions is the most appropriate thing to do in current GNSS receivers when using dual polarized antennas. Nevertheless, when the LOS is present we can do better trying to reduce the effects of multipath into the obtained measure. To do so, three different concepts were proposed in [9], namely measurement weighting, range and tracking correction. So, whenever NLOS signals are detected (exclusion area) these should be discarded from the navigation solution. The rest of signals should be used after applying some multipath countermeasure. In this paper we will focus on the measurement weighting solution. The main idea of this countermeasure is that the effects of multipath into the PVT solution can be reduced by estimating the standard deviation of the range measures due to multipath and pass it to the navigation processor, so that the measures can be weighted accordingly.

In particular, in order to estimate the standard deviation of the measurements we will use an experimental model based on the RHCP and LHCP components, namely

$$\sigma = f\left(P_{\mathrm{L}}, P_{\mathrm{R}}, \mathrm{CN0}_{\mathrm{R}}; a, b\right), \tag{1}$$

where P_{L} and P_{R} stand for the prompt correlator value of the LHCP and RHCP component, respectively, $\mathrm{CN0}_{\mathrm{R}}$ the carrier-to-noise ratio (CN0) of the RHCP component, and $\{a, b\}$ are the model parameters. The form of the model (i.e. $f(\cdot)$) may be derived theoretically, but the parameters have to be determined empirically. Doing so we will take into account several practical aspects such as receiver design and/or antenna artifacts. A proper model may be of the form

$$f\left(P_{\mathrm{L}}, P_{\mathrm{R}}, \mathrm{CN0}_{\mathrm{R}}\right) = \sigma_0(\mathrm{CN0}_{\mathrm{R}}) \cdot \left[1 + c_1 \cdot \frac{P_{\mathrm{L}}}{P_{\mathrm{R}}}\right] + c_2, \tag{2}$$

where $\{c_1, c_2\}$ are two constants, and $\sigma_0(\cdot)$ the traditional model for the standard deviation used for CN0- or elevation-based weighting [13], [14].

The idea in (2) is to add a correction factor to the traditional weighting models. This correction factor increases as long as the LHCP to RHCP ratio increases, thus increasing the modeled standard deviation as long as the multipath effects are stronger (with respect to the LOS signal). This concept is similar as the one adopted in [15] and [16] in order to model NLOS and ionospheric errors, respectively. Specifically, we consider the following model:

$$\begin{aligned}\sigma^2 &= a \cdot \frac{1}{\mathrm{CN0}_{\mathrm{R}}} \cdot \left[1 + c \cdot \frac{P_{\mathrm{L}}}{P_{\mathrm{R}}}\right] \\ &= a \cdot \frac{1}{\mathrm{CN0}_{\mathrm{R}}} + b \cdot \frac{P_{\mathrm{L}}}{\mathrm{CN0}_{\mathrm{R}} \cdot P_{\mathrm{R}}},\end{aligned} \tag{3}$$

with σ the standard deviation of the measurement error. From (2), we have used $c_1 = c$ and $c_2 = 0$ in (3) and the traditional CN0 weighting model.

As already stated, the model parameters $\{a, b\}$ should be determined empirically. Specifically, in order to include a proper correction factor, a two-dimensional optimization will be considered. This is for making sure that the correction factor included in (3) increases when the multipath effects are stronger and not because any other effect such as signal attenuation. This fact is illustrated in Fig. 8 in which we see how for a given value of CN0 in the RHCP component we have different pseudorange errors depending on the scenario we are. Similar behavior is experienced with the phase error. This difference of error for a given RHCP CN0 value is mainly due to the multipath effects (scenario dependent), which will be visible in the LHCP component. For this reason, a two-dimensional or equivalently a 3D-shape fitting will be performed. This is illustrated in Fig. 9 in which the shaded-shape is the resulting fitting after estimating the model parameters in (3) using the empirical data showed as the colored-shape.

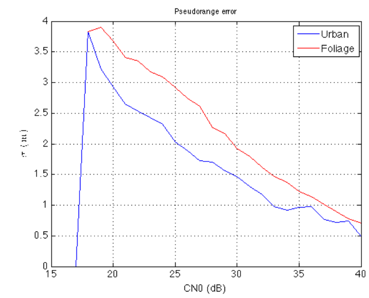

Fig. 8. Comparison of the pseudorange error as a function of the CN0 for different scenario. The gap between curves is due to multipath effects to be modeled through the LHCP component.

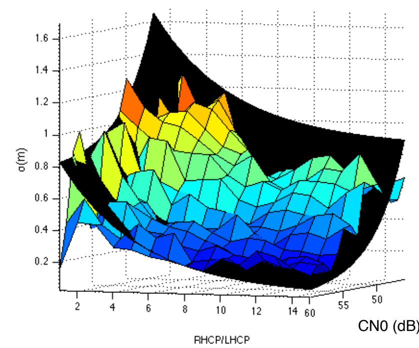

Fig. 9. Least-Squares 3D fitting of the measured phase errors as a function of the RHCP to LHCP ratio and the CN0 of the RHCP component. Empirical data (colored) and fitted shape (black).

Before estimating the model parameters, let us first talk about the empirical computation of the range errors. Indeed, both pseudorange and phase measurements should be analyzed. In order to empirically compute the measurement errors, for the pseudorange, we use the traditional code-minus-carrier (CMC) iono-free combination. For the phase error, let us define the residual phase error, ϵ_{r}, as the difference between the measured phase, ϕ_{m}, and the one obtained from the estimated PVT solution, $\widetilde{\phi}$. Then, we have

$$\epsilon_{\mathrm{r}} \doteq \phi_{\mathrm{m}} - \widetilde{\phi} = \phi_{\mathrm{m}} - \widetilde{\phi} + \phi - \phi = \epsilon_{\phi} + \phi - \widetilde{\phi}, \tag{4}$$

with ϕ the real phase and $\epsilon_{\phi} \doteq \phi_{\mathrm{m}} - \phi$ the phase measurement error. It is worth pointing out that the term $\phi - \widetilde{\phi}$ is equivalent to the projection of the error vector, $\boldsymbol{\epsilon}$, into the truth range vector, $\widehat{\boldsymbol{\rho}}$. So, we can compute the real phase error as

$$\epsilon_{\phi} = \epsilon_{\mathrm{r}} - \boldsymbol{\epsilon}^{\top} \cdot \widehat{\boldsymbol{\rho}}, \tag{5}$$

where $\boldsymbol{\epsilon}$ is the 3D vector given by the difference between the estimated PVT and the real position, and $\widehat{\boldsymbol{\rho}}$ is the unitary vector of the

TABLE I
RELATIVE IMPROVEMENT IN TERMS OF RMS 3D ERRORS. IMPROVEMENT OF APPLYING DUAL POLARIZATION EXCLUSION.

Scenario	Relative improvement RMS 3D error
Static_Foliage	3%
Static_Urban	50%
Dynamic	11%

direction between the real position and the satellite. Summarizing, to compute the phase error, we use the phase residual error minus the projection of the PVT error into the truth range.

Once both pseudorange and phase measurement errors are calculated, the next step is to estimate the model parameters from this data. For the sake of notation simplicity, let us define $x_i \doteq \mathrm{CN0_R}(i)$ and $y_i \doteq P_\mathrm{L}(i)/P_\mathrm{R}(i)$ with $i = 1, \ldots, N$ the measurement index. Let also $\sigma^2(i)$ be the measured root mean square (RMS) error of the range measurements. Therefore, from (3), we can write

$$\boldsymbol{\sigma}^2 = \begin{bmatrix} \sigma^2(1) \\ \sigma^2(2) \\ \vdots \\ \sigma^2(N) \end{bmatrix} = \begin{bmatrix} \frac{1}{x_1} & \frac{y_1}{x_1} \\ \frac{1}{x_2} & \frac{y_2}{x_2} \\ \vdots & \vdots \\ \frac{1}{x_N} & \frac{y_N}{x_N} \end{bmatrix} \cdot \begin{bmatrix} a \\ b \end{bmatrix} = \boldsymbol{H} \cdot \boldsymbol{\theta}, \tag{6}$$

and the model parameters can thus be estimated by a least-square fitting as

$$\widehat{\boldsymbol{\theta}} = \begin{bmatrix} \widehat{a} \\ \widehat{b} \end{bmatrix} = (\boldsymbol{H}^\top \boldsymbol{H})^{-1} \boldsymbol{H}^\top \cdot \boldsymbol{\sigma}^2. \tag{7}$$

Then, the standard deviation to feed the PVT engine at time n can be estimated as a function of x_n and y_n by

$$\widehat{\sigma}(n) = \sqrt{\widehat{a} \cdot \frac{1}{x_n} \cdot \left(1 + \frac{\widehat{b}}{\widehat{a}} \cdot \frac{y_n}{x_n}\right)}. \tag{8}$$

IV. PVT RESULTS

In the previous sections we have demonstrated the capability of the dual polarized antenna to detect the presence of NLOS (see Fig. 7) and to provide a good match between the proposed measurement weighting and the measured error standard deviations (see Fig 9). Now, it is time to see the effects of exploiting these capabilities on the performance of the PVT solution. In particular, at each scenario, the RHCP and LHCP I/Q correlation data were stored as well as the traditional measurements of the GNSS receiver for the RHCP component. Those included measurements such as the CN0, pseudorange, carrier phase, and navigation data. These were used along with RTCM3 streams from a nearby reference station for position calculation. This was done with a modified version of Septentrio's commercial post-processing tool. This tool was first calculating the position in the regular way based on the RHCP measurements. In a second run, the position was recalculated making use of polarization information. The multipath and noise related component of the error model of the positioning engine were overruled with the polarization-based model as discussed, while excluding ranges with excessive LHCP/RHCP ratio. All constellations available were used for the PVT computation.

The true position was known in all tests. This was used to calculate the error statistics of the regular and polarization-enhanced positioning solution. We show in Table I the relative improvement (in terms of RMS 3D error) of using the dual polarized antenna, with respect to the regular configuration. We see how the positioning performance in terms of RMS 3D error is improved with the use of the dual polarized antenna. This improvement is not big in the foliage and dynamic scenarios, a reduction of 3% and 11% of the 3D error, respectively. Nevertheless, this is not the case in the static urban scenario, in which the dual polarization configuration provides a reduction of almost 50% of the original error. The reason of these results can be explained by the type of NLOS propagation in each scenario. It is known that a long delay (distant reflector) introduce a large position error, whereas a short path delay (near reflector) have a much smaller effect. It is likely that the NLOS propagation in the static urban scenario comes from distant reflectors, thus causing large errors. This fact would explain the large improvement in the urban scenario, with respect to the foliage scenario, in which the reflections might come from near reflectors.

TABLE II
PERCENTAGE OF TIME IN RTK FIXED MODE.

Scenario	RTK Fixed (% of time)	
	1 antenna	2pol exclusion
Static_Foliage	29	19
Static_Urban	85	85
Dynamic	61	62

TABLE III
RMS 3D ERRORS IN THE RTK FLOAT MODE WHEN APPLYING DUAL POLARIZATION EXCLUSION (2POL EXCLUSION) OR NOT (1 ANTENNA).

Scenario	RTK Float RMS 3D error (cm)	
	1 antenna	2pol exclusion
Static_Foliage	213	186
Static_Urban	80	37
Dynamic	96	88

It is worth pointing out that the presented results were obtained using RTK phase-based positioning, thus providing high-accuracy performance around 5 cm to 2 m for the fixed and float RTK mode, respectively. The percentage of time that the receiver is able to fix the phase ambiguities is shown in Table II. The percentage of time in RTK fixed mode is particularly high in the urban scenario, being greater than 80%, and dynamic scenario, which is more than the 50%. The rest of time the receiver is operating in RTK float mode, except in the dynamic scenario in which a 20% of the time the receiver is in Standalone mode. This distribution of errors and percentage of time is the reason of the difference of the improvement in terms of RMS error between scenarios. Another explanation of these results is the fact that the accuracy of the position solution obtained after excluding signals depends on the quality of the remaining signals and the quality of the user-satellites geometry.

For instance, results in Table II show how the application of the exclusion function do not improve the percentage of time that the receiver is working with RTK fixed mode, being even worse in the foliage scenario. The reason is that in this scenario most signals were contaminated by multipath, NLOS reception and/or diffraction. In such a case, when excluding signals, the quality of the remaining signals might be worse than the excluded ones, being thus more difficult for the receiver to fix the phase ambiguities. As a result, in the foliage scenario, those epochs that the receiver is not able to fix the ambiguities become in float mode. On the contrary, in the urban scenario, there were several signals with good visibility and few signals with severe multipath (see Fig. 7). Thus, when excluding the severe multipath we improve the accuracy because we have

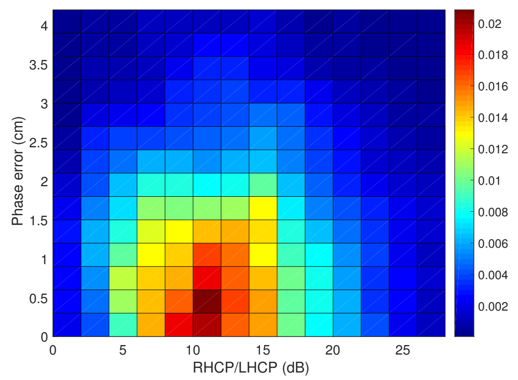

Fig. 10. Relative frequency of the phase error measurements as a function of the RHCP to LHCP ratio.

good signals with good geometry. Nevertheless, this accuracy is not reflected in an improvement of the resolution of phase ambiguities, which is maintained, but in the reduction of the RTK float mode error. Similar arguments hold for the dynamic scenario.

So, in general, the improvements on the positioning performance shown in Table I come from the improvements on the RTK float mode error. The RMS 3D errors for the RTK float mode for all the analyzed scenarios are collected in Table III. Finally, it is worth noting that the results that we have presented in this section were obtained only applying the exclusion function. This is because the application of the weighting function did not provide a valuable effect into the PVT solution. The reason is explained with the results in Fig. 10, which shows the relative frequency of the phase error as a function of the RHCP to LHCP ratio. That is, the percentage of measurements that lies in a given grid of error for a given value of RHCP to LHCP ratio. We see in the figure that we have small errors even for small values of the RHCP-LHCP ratio, and viceversa. With this kind of behavior is difficult that the used weighting function provides a proper fit useful to improve the positioning performance.

V. Conclusions

A novel weighting and exclusion function has been proposed and demonstrated using real data collected within the framework of the FANTASTIC project. The technique uses the RHCP and LHCP components of a dual polarized antenna. Depending on the difference between the strength of these two components, the technique decides whether to exclude or weight the measurements. We have demonstrated the detection of NLOS and the improvement of removing these signals from the PVT computation. For the first time, we have assessed the effects of this exclusion into the RTK phase-based positioning. In general, we can conclude that exclusion is beneficial for RTK positioning because the RMS 3D error is reduced. It is worth noting, though, that this improvement is dependent on the scenario. Actually, the improvement depends on the NLOS propagation (i.e. small or large delay) and the quality of the remaining signals and user-satellite geometry.

It is for the above reason that, as indicated by the obtained results, the exclusion function is very useful in urban environments or those environments with large delay NLOS propagation and/or scenarios in which most signals have good visibility and there are few signals with severe multipath. Regarding the weighting function, we have proved a good fitting between the used model and the measured data. Notwithstanding, this fitting was not translated into a valuable improvement of the PVT solution. The reason is that in RTK phased-based positioning the phase measurements used for the PVT computation are accurate measurements with similar errors (of the order of few cm). Then, the weights provided by the weighting function will be similar, thus the effects on the PVT solution will be negligible.

Acknowledgment

This work was partly supported by the Spanish Grant TEC2017-89925-R and by the European GNSS Agency (GSA) under the FANTASTIC project (GSA/GRANT/01/2016). The authors would also like to thank GMV and Instituto Superiore Mario Boella (ISMB), as part of the consortium that carried out the FANTASTIC project, for their valuable support.

References

[1] M. S. Braasch, "Performance comparison of multipath mitigating receiver architectures," in *Proceedings of the IEEE Aerospace Conference*, vol. 3, 2001, pp. 3–1309.

[2] M. Z. H. Bhuiyan, E. S. Lohan, and M. Renfors, "Code tracking algorithms for mitigating multipath effects in fading channels for satellite-based positioning," *EURASIP Journal on Advances in Signal Processing*, vol. 2008, no. 1, pp. 1–17, 2007.

[3] L. Lau and P. Cross, "Development and testing of a new ray-tracing approach to GNSS carrier-phase multipath modelling," *Journal of Geodesy*, vol. 81, no. 11, pp. 713–732, 2007.

[4] E. Shytenneja, A. Garcia-Pena, and O. Julien, "Proposed architecture for integrity monitoring of a GNSS / MEMS system with a fisheye camera in urban environment," in *Proceedings of the International Conference on Localization and GNSS (ICL-GNSS)*, 2014, pp. 1–6.

[5] N. Vagle, A. Broumandan, A. Jafarnia-Jahromi, and G. Lachapelle, "Performance analysis of GNSS multipath mitigation using antenna arrays," *The Journal of Global Positioning Systems*, vol. 14, no. 1, p. 4, 2016.

[6] C. Yang and C. A. Porter, "GPS Multipath Estimation and Mitigation Via Polarization Sensing Diversity : Parallel Iterative Cross Cancellation," in *ION GNSS 18th International Technical Meeting of the Satellite Division*, 2005, pp. 2707–2719.

[7] D. Manandhar, R. Shibasaki, and H. Torimoto, "GPS Reflected Signal Analysis using Software Receiver," *Journal of Global Positioning Systems*, vol. 5, no. 12, pp. 29–34, 2006.

[8] M. Brenneman, J. Morton, C. Yang, and F. van Graas, "Mitigation of GPS multipath using polarization and spatial diversities," in *Proceedings of the 20th International Technical Meeting of the Satellite Division of The Institute of Navigation (ION GNSS 2007)*, 2007, pp. 1221–1229.

[9] P. D. Groves, Z. Jiang, B. Skelton, P. A. Cross, L. Lau, Y. Adane, and I. Kale, "Novel multipath mitigation methods using a dual-polarization antenna," in *Proceedings of the annual meeting of the Institute of Navigation (ION GNSS+)*, 2010, pp. 140–151.

[10] P. D. Groves, Z. Jiang, M. Rudi, and P. Strode, "A portfolio approach to NLOS and multipath mitigation in dense urban areas," in *26th International Technical Meeting of the Satellite Division of the Institute of Navigation, ION GNSS 2013*, 2013, pp. 3231–3247.

[11] Z. Jiang and P. D. Groves, "NLOS GPS signal detection using a dual-polarisation antenna," *GPS Solutions*, vol. 18, no. 1, pp. 15–26, 2014.

[12] K. Palamartchouk, P. Clarke, and S. Edwards, "Mitigation of GNSS multipath by the use of dual-polarisation observations," *RICS Research*, no. July, p. 32, 2014.

[13] J. Li and M. Wu, "The improvement of positioning accuracy with weighted least square based on SNR," in *Proceedings - 5th International Conference on Wireless Communications, Networking and Mobile Computing, WiCOM 2009*, 2009, pp. 9–12.

[14] H. Hartinger and F. K. Brunner, "Variances of GPS Phase Observations: The SIGMA- Model," *GPS Solutions*, vol. 2, no. 4, pp. 35–43, 1999.

[15] S. Tay and J. Marais, "Weighting models for GPS Pseudorange observations for land transportation in urban canyons," in *Proceedings of 6th European Workshop on GNSS Signals and Signal Processing*, 2013, pp. 1–6.

[16] D. Odijk, "Weighting Ionospheric Corrections to Improve Fast GPS Positioning Over Medium Distances," in *ION GPS*, no. August, 2000, pp. 1113–1123.